Cuadernos de Investigación Geográfica *Geographical Research Letters*	2023	Nº 49 (2)	pp. 65-81	EISSN 1697-9540

http://doi.org/10.18172/cig.5523

ASSESSMENT OF LAND DEGRADATION AND DROUGHTS IN AN ARID AREA USING DROUGHT INDICES, MODIFIED SOIL-ADJUSTED VEGETATION INDEX, AND LANDSAT REMOTE SENSING DATA

ABDESSAMED DERDOUR [1], ANTONIO JODAR-ABELLAN[2,3*], AMPARO MELIAN-NAVARRO[4], RYAN BAILEY[5]

[1]*University Center Salhi Ahmed Naama (Ctr Univ Naama), Department of Natural and Life Sciences, Laboratory for the Sustainable Management of Natural Resources in Arid and Semiarid Zones, Algeria.*

[2]*Spanish Research Council, Centro de Edafología y Biología Aplicada del Segura (CEBAS-CSIC), Soil and Water Conservation Group, Murcia, Spain.*

[3]*University Institute of Water and Environmental Sciences. University of Alicante, Spain.*

[4]*Cartography Engineering and Graphic Expression in Engineering Department, Agro-Environmental Economics, Miguel Hernández University of Elche, 03312 Orihuela, Spain.*

[5]*Department of Civil and Environmental Engineering, Colorado State University (USA).*

ABSTRACT. Ain Sefra is part of the Ksour Mountains and it's situated in southwestern Algeria, where the climate is arid. The study area is progressively facing regression and degradation exacerbated by climate change. These trends point to a significant acceleration of desertification and drought and the loss of production systems that play a critical social, ecological, and economic role in the region. To better understand the natural hazard of dryness in Ain Sefra and the impact of climate change, we used various drought indices and remote sensing data. Hence, analyzing precipitation records from 1965 to 2021, through several drought indices, droughts were identified as a recurring phenomenon. Moreover, the frequency of successive dry years is relatively high. There were three most extended continuous dry periods. The first phase lasted seven years from 1980 to 1987, the second twelve years from 1994 to 2006, and the third nine years from 2012 to 2021. Calculation of the Modified Soil-Adjusted Vegetation Index (MSAVI) for five multidate satellite images allowed us to follow the evolution of land use elements in this region from 1977 to 2017. Indeed, the study of these multi-temporal images reveals a considerable growth of sands, moving towards the north and northeast of the zone during the last decades. The combination of drought indices and remote sensing seems to be most promising; whose results are valuable tools for guidance and decision support to local and regional authorities.

Evaluación de la degradación del suelo y sequías en una región árida utilizando índices de sequía, índice de vegetación ajustado al suelo modificado y datos de sensores remotos Landsat

RESUMEN. Ain Sefr, en las montañas Ksour, está situada en el suroeste de Argelia, donde el clima es árido. El área de estudio se enfrenta progresivamente a la regresión y degradación exacerbada por el cambio climático. Estas tendencias apuntan a una aceleración significativa de la desertificación y la sequía y a la pérdida de sistemas de producción que desempeñan un papel social, ecológico y económico crítico en la región. Para comprender mejor el peligro natural de la sequía en Ain Sefra y el impacto del cambio climático, se varios índices de sequía y datos de

teledetección. Al analizar los registros de precipitación desde 1965 hasta 2021, a través de varios índices de sequía, se identificaron las sequías como un fenómeno recurrente. Además, la frecuencia de años secos sucesivos es relativamente alta. Hubo tres períodos secos continuos más prolongados. La primera fase duró siete años, de 1980 a 1987, la segunda doce años, de 1994 a 2006, y la tercera nueve años, de 2012 a 2021. El cálculo del Índice de Vegetación Ajustado al Suelo Modificado (MSAVI) para cinco imágenes satelitales multifecha nos permitió seguir la evolución de los elementos de uso del suelo en esta región desde 1977 hasta 2017. De hecho, el estudio de estas imágenes multitemporales revela un crecimiento considerable de arenas, moviéndose hacia el norte y noreste de la zona durante las últimas décadas. La combinación de índices de sequía y sensores remotos parece ser muy prometedores, pues sus resultados son valiosas herramientas de orientación y apoyo a la decisión de los entes locales y regionales.

Keywords: Ain Sefra, MSAVI, Dry climate, Drought, Sustainability.

Palabras clave: Ain Sefra, MSAVI, Clima seco, Sequía, Sostenibilidad.

Received: 28 July 2022

Accepted: 14 January 2023

***Corresponding author:** Antonio Jodar-Abellán. Spanish Research Council, Centro de Edafología y Biología Aplicada del Segura (CEBAS-CSIC), Soil and Water Conservation Group, Murcia, Spain. E-mail address: ajodar@cebas.csic.es

1. Introduction

Climate change has been reported worldwide in recent years (e.g., Ripple *et al.,* 2021; Tahir *et al.,* 2021; UN, 2022). Because of the increased intensity and frequency of severe events such as droughts, heatwaves, sandstorms, forest fires, and floods, scientists are now focusing on the effects of climate change (e.g., Corwin, 2021; Malhi *et al.,* 2021; Niñerola *et al.*, 2020; Camarasa-Belmonte, 2021; Rodrigo-Comino *et al.,* 2022; Eekhout *et al.,* 2021). Droughts are one of the most complicated extreme climatic situations, affecting more people than any other hazard or natural disaster (Wilhite, 2000; Oliveira-Santos *et al.,* 2022; Mendoza-Uribe, 2022). The impacts of droughts have generally been referred to as direct impacts, such as reducing vegetation cover and decreasing soil and vegetation water content (Van Leeuwen *et al.,* 2019; Valdes-Abellan *et al.,* 2020; Palacios-Cabrera *et al.,* 2022; Silva *et al.,* 2022). Therefore, lower crop productivity, less water reservoirs, deterioration in the number of herds, increases in the risk of fires are identified (Fadhil, 2011). If the current year is succeeded by one or more dry years, the drought's severity is felt. In addition, a series of consecutive dry years is more severe than a singular drought (Spinoni *et al.,* 2014; Jodar-Abellan *et al.,* 2019). Drought is a lack of precipitation for an extended period, usually a season or more, resulting in water scarcity affecting agricultural or environmental activities (Mishra and Singh, 2010; Cámara-Artigas *et al.,* 2022; Juárez *et al.,* 2022). Thus, drought is a progressive process that begins with a lack of rainfall, expressed as meteorological drought. It can be classified into four categories: meteorological, agricultural, hydrological, and socioeconomic (Eklund and Seaquist, 2015). Meteorological droughts are also the source of hydrological droughts (Spinoni *et al.,* 2014; Jodar-Abellan *et al.,* 2018). Agricultural droughts depict severe decrease in soil water that results in crop failure. Drought can worsen, resulting in a so-called socioeconomic drought. Its prevalence is linked to natural water reserves, and reservoirs constructed by human when storage cannot meet the demand for water (Guo *et al.,* 2019; Boix-Fayos *et al.,* 2020; Eekhout *et al.,* 2020). As a result, if appropriate safeguards are not taken, it will severely impact economies of the affected regions. Drought features must be accurately estimated to plan for optimal water resource usage and agricultural productivity (Kogan and Guo, 2016).

More than 100 drought indices are used to determine drought globally (Jain *et al.,* 2015). Among all the standardized drought indices, McKee *et al.* (1993) presented the Standardized Precipitation Index (SPI), which is widely used to identify drought in various regions throughout the world (Li *et al.,* 2020; Sobral *et al.,* 2019; Stagge *et al.,* 2015; Tsakiris and Vangelis, 2004). SPI is recommended because it only uses precipitation and is straightforward to calculate at various periods. It also characterizes short- and long-term meteorological and agricultural droughts (Golian *et al.,* 2015). The SPI is directly tied to soil water on short durations, but it can also be related to groundwater and reservoir storage on longer timelines (Keyantash, 2018). According to IPCC assessments, the Mediterranean basin, particularly North Africa, is one of the most vulnerable regions to climate change (Wang, 2005). However, there is a scarcity of data on the North African region (UN, 2022; Derdour *et al.,* 2020). Analysis of remote sensing data can support continuity meteorological data and indices by filling gaps that can occur in long time series, as well as providing a wealth of information about vegetation, soil status, and land use, which is frequently used in drought studies to quantify the growth and degradation of various land use items in response to climatic factors (dry and wet periods) and human activities. Therefore, remote sensing became an alternative to collect information that is challenging to obtain by other means. Over the last decade, data from various satellite-based platforms have figured prominently in drought research (e.g., AghaKouchak *et al.,* 2015; West *et al.,* 2019). Furthermore, advancements in algorithm improvement as well as cloud-based processing and storage capacity have significantly expanded the potential application of remote sensing for drought research. In addition to providing an autonomous experimental capability, remote recognizing data can be used to minimize doubts and constrain modeling efforts aimed at drought estimates. During last years, numerous studies have been published on drought monitoring and its ramifications such as desertification, soil loss, sand dune mobility (e.g., AghaKouchak *et al.,* 2015; Bouarfa *et al.,* 2022a; Wardlow *et al.,* 2012; West *et al.,* 2019; Rahdari and Rodríguez-Seijo, 2021; Zhang and Jia, 2013; Ibañez *et al.,* 2022; Cimusa-Kulimushi *et al.,* 2023).

Drought is one of the most concerning manifestations of climate change in Algeria. Several droughts had previously occurred before the start of the twentieth century, in the 1940s, and the 1970s resulting in low harvests, animal losses, and increased food prices (Seltzer, 1946). Droughts in recent years have been even more notable for their geographic scope and ferocity. They were characterized by rainfall shortages that significantly reduced monthly mean flows (Bouabdelli *et al.,* 2020; Habibi *et al.,* 2018; Lazri *et al.,* 2015). In this work, drought episodes in the region of Ain Sefra, which is located in southwest Algeria, were studied using drought indices such as the previously mentioned SPI, the precipitation mean deviation index (MDX), the rainfall index (RI), the Frequency analyses (FI), and the standard deviations Indicator (SDI). These indices were used at various time scales (1, 3, 6, 9, and 12 months) from a database of the only rainfall station situated in the city, over 56 years (1965-2021), summarizing 672 monthly precipitation series. On the other hand, a diachronic study using remote sensing was conducted to reconstruct the evolution of the sand mobility and vegetation cover in Ain Sefra between 1977 and 2017 using the Modified Soil-Adjusted Vegetation Index (MSAVI). This research aims to understand better the impact of climate change and management methods on these vulnerable areas, detect dry and wet periods in Naâma (Argelia), and then assess their trends over time.

2. Materials and Methods

2.1. Study area

This study was conducted in southwestern Argelia in the Ain Sefra region (Fig. 1: 32°30'00″N / 33°00′0″N and 0°50′0″W / 0°20′0″W), covering an area of 13,409 km^2, in the high plains of southern Oran. The case study area is located in western Algeria, between the Tell and Saharan Atlases, in the "Ksour Mountains" region, highly affected by droughts (Haddouche *et al.,* 2008). The study area is composed by sets of massifs with complex structures that are elongated and stretched along the general axis of the southwest/north- east fold (Derdour *et al.,* 2020). These structures are generally related to tectonics, lithology, and erosion. They are made up of hard rocks (limestone, dolomitic limestone and

sandstone) of Jurassic age, whose slopes are generally steep (Derdour *et al.,* 2020). Among these folded formations, the Jurassic anticline culminates at 2236 m a.s.l. in a southwest/northeast direction (Derdour *et al.,* 2017a). The study area is situated in the Wilaya of Naâma, mainly occupied by a flat plain. The altitude increases significantly towards the South (1000 to 1330 m a.s.l.). It is riddled with many small basins of different sizes and origin (Sebkha, Dayas, hydro-wind basins locally called Mekmene, Oglat or Haoud). We distinguish between the salty pits (Chott Chergui, Chott El Gharbi, Sebkha de Nâama) and the Dayas and the Mekmenes, where unsalted surface water accumulates (Bouarfa *et al.,* 2022b). Dayas soils are generally deeper compared to encrusted glacis. The Chotts and the Sebkhas are salty depressions resulting in a steppe with halophytes. Throughout the Algerian steppe and the pre-Saharan region, multiple traces of wind activity increasingly underline the arid facies of the landscape. Therefore, wind is the fundamental element in shaping semi-arid, infertile, and desert landscapes. The hydrographic network in the study area is endorheic (Derdour and Bouanani, 2019). It is poorly developed and often emerges in areas of evaporation such as Dayas or Sebkhas. The valleys are however quite short, not very sinuous, showing a flat bottom and badly drawn banks. This explains the low slope of the river and the presence of endorheic basins (dayas). Hydrologically, the valleys are not perennial and only flow episodically during rainy periods (Derdour *et al.,* 2017a).

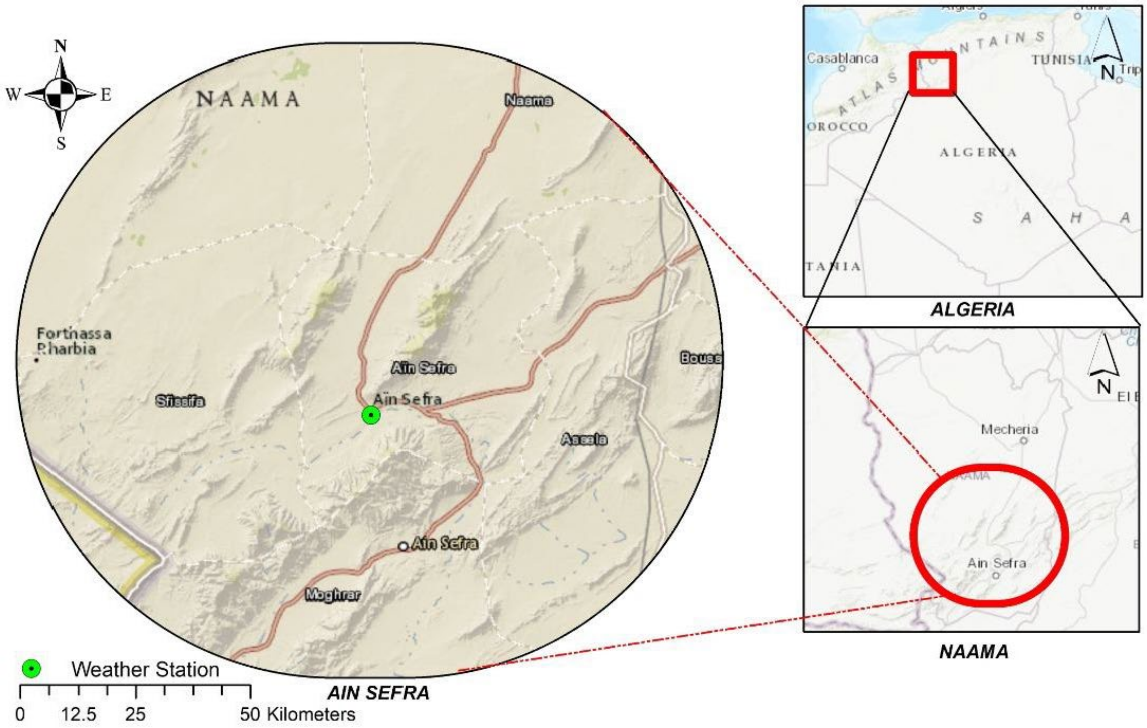

Figure 1. Study area.

2.2. Data collection

The precipitation dataset from 1965 to 2021 at Ain Sefra, run by the National Office of Meteorology of Algeria, was used. The climatic data was processed, and the homogeneity of the climatic series was verified. It should be noted that missing data were downloaded from the IOWA State University website (IOWA, 2022). The considered weather station is located at 722729.00 UTMx and 3627490.00 UTMy and depicts a mean altitude of 1084 m a.s.l.

Five satellite images type Landsat 2 Multispectral Scanner System were used to get images of the year 1977, Landsat 3 Multispectral Scanner System , and Thematic Mapper (TM) to get images of

the year 1987, Landsat 5 Multispectral Scanner System and Thematic Mapper to get images of the year 1997, Landsat 7 Enhanced Thematic Mapper Plus Instrument to get images of the year 2007, and Landsat 8 Operational Land Imager and Thermal Infrared Sensor to get images of the year 2017 of the study area , downloaded from the US Geological Survey website (USGS, 2022). They allowed for diachronic research in the study area and the detection of changes using remote sensing, a technique for identifying the various states of an object or phenomena when monitored over time. These satellite images from different years (1977, 1987, 1997, 2007, and 2017) were chosen to conduct this comparison study. The selected satellite images were taken in March of every year, around the same time. A post-classification technique performed change detection analysis of multidate satellite images. The Landsat TM data pre-processing in this work contains multiple correction techniques that are carried out in several steps, including radiometric correction, FLAASH atmospheric correction, supervised classification, post-classification, and geometric corrections.

2.3. Drought indices

2.3.1. Standardized Precipitation Index (SPI)

The SPI is a multi-scalar stochastic predictor that assesses precipitation deficit during wet and dry spells and allows for drought monitoring on multiple time scales (McKee *et al.,* 1993). This indicator was proposed by the World Meteorological Organization as a jumping-off place for rainfalls monitoring. It has been utilized in numerous prior researches due to its simplicity, and widespread acceptance. The computation is carried out with the help of monthly rainfall data which has been adapted to a probability density function such as gamma over a lengthy period. Any percentile from the chosen distribution model is handled as a percentile on a Gaussian distribution function, and the appropriate Z value is recorded as the SPI value.

The SPI is calculated by fitting a probability density function to the frequency distribution of precipitation accumulated across the time scale of interest. This is done for each month (or any other temporal basis of the raw precipitation time-series as required) and each place in space individually. The normalized normal distribution is then applied to each probability density function. The probability density function of the gamma distribution is as follows (Eq.1):

$$g(x) = \frac{1}{\beta^{\alpha}T(\alpha)} x^{\alpha-1} e^{-x/\beta} \; for \; x > 0 \qquad (1)$$

where x is precipitation, α>0 is the shape e parameter, and β>0 is the scale parameter.

The gamma probability density function parameters are estimated at the data location for each time scale and observation. To estimate α and β parameters, maximum likelihood solutions are utilized (Edwards, 1997; Thom, 1966). The SPI is defined as (Eq.2):

$$SPI = \frac{P_i - P_m}{\sigma} \qquad (2)$$

where: P_i is the annual rainfall for a given year (mm), P_m the mean rainfall (mm), and σ the standard deviation. The data are then used to calculate drought characteristics such as duration, intensity, and severity. Moderate, severe, and extreme drought situations are indicated by ranges of -1.49 to -1.0, -1.5 to -1.99, and ≤−2.0. Various classifications of drought intensity based on SPI thresholds are available (McKee *et al.,* 1993).

2.3.2. Precipitation Mean Deviation Index (MDX)

The MDX (Eq.3) is the variation between both the annual precipitation level (P_i) and the average rainfall level (P_m).

$$MDX = P_i - P_m \quad (3)$$

The yearly distribution of precipitation offers immediate information on the variability of rainfall rates. It is easy to distinguish the wet and dry years by comparing it to the series average. It also makes it possible to estimate the precipitation shortage at the year's level and picture and establish the number of shortfall periods and their sequence. A deficit year is one in which the precipitation is less than the mean, and a surplus year is when the standard is exceeded.

2.3.3. Rainfall Index (RI)

The RI reflects how much precipitation is collected in comparison to the long-duration mean designed for a certain place and timeframe. The rainfall index *RI* is defined as (Eq.4):

$$RI \quad = P_i / P_m \quad (4)$$

In particular, if this ratio is more than one, the year is characterized as wet, and as dry if it is less than one. We have used the difference relative to the norm (R_{IM}), to identify rainfall in a lengthy set of rainfall records (Eq.5).

$$R_{IM} = RI \quad - 1 \quad (5)$$

The cumulative of the indices (R_{IM}) of successive years makes it possible to identify the main trends by disregarding the slight fluctuations from one year to the next. It is a wet trend when the total of the indexes rises and a dry trend forthe opposite scenario (Bergaoui and Alouini, 2002).

2.3.4. Frequency analyses (FI)

Frequency analyses are commonly used based on the characteristics of a phenomenon such as droughts. Annual rain is classified in increasing order based on their chance of not surpassing (F), which is calculated as follows (Eq.6):

$$F = \left(\frac{r}{N+1}\right).100 \quad (6)$$

where *r* is the ranking of the year based on an increasing categorization of rainfall quantities; *N* is the number of years of monitoring. Years are categorized into five groups of likelihoods of non-exceedance, as shown in Table 1.

Table 1. Classification of frequency.

Class	Frequency
Very dry	F < 15%
Dry	15% ≤ F < 35%
Normal	35% ≤ F <65%
Wet	65% ≤ F < 85%
Very wet	85% ≤ F

2.3.5. Standard deviations Indicator (SDI)

This index is measured by considering the annual rainfall mean readings (P_m) in relation to the value of standard deviations (σ) whose formulation is as follows (Eq.7, Bergaoui and Alouini, 2002):

$$\sigma = \left[\frac{1}{(N-1)}\right]\sum(P_i - P_m)^{1/2} \quad (7)$$

when P_i is less than P_m-σ, serious droughts are identified. However, if P_i is a smaller amount than P_m-2σ the drought is severe, as depicted in Table 2.

Table 2. Drought severity classes.

Type of drought	**Comparison criterion**
Moderate	$P_m - \sigma < P_i < P_m$
Strong	$P_m - 2\sigma < P_i < P_m - \sigma$
Very strong	$P_i < P_m - 2\sigma$

2.4. Diachronic analysis using Remote Sensing

In this study, we used Landsat satellite images to understand the change observed in sand and vegetation cover. Hence, we tested statistically the "change detection" technique over 40 years (between 1977 and 2017) by using an index that considers soil influence called the Modified Soil-Adjusted Vegetation Index (MSAVI). This index, proposed by Qi et al. (1994), suggests an enhancement to the original soil-adjusted vegetation index (SAVI). In particular, the L-shaped adjustment parameter that characterizes the soil and its vegetation cover rate in the MSAVI is no longer a constant, but it is automatically adjusted to local conditions. This index has been widely used in the low vegetation zone, as in the case of our study area. MSAVI is determined as a ratio of the R (red) and NIR (near infra-red) wavelengths values with an inductive L function utilized to amplify the lessening of soil influences on the flora signal.

Likewise, MSAVI values range from -1 to 1, where i) -1 to 0.2 indicate bare soil; ii) 0.2 to 0.4 is the seed germination stage; and iii) 0.4 to 0.6 is the leaf development stage.

3. Results and Discussion

3.1. Drought indices

3.1.1. Standardized Precipitation Index (SPI)

The rainfall index was calculated to characterize precipitation deficiencies at various time periods in a specific location. This analysis, which considers the futility of time, mainly reflects drought's influence on the availability of numerous water supplies. Droughts receive a negative rating, whereas floods receive a positive value. The SPI of the study area was calculated by fitting rainfall series collected over 56 years from 1965 to 2021 (McKee *et al.,* 1993). The chronological variation of the SPI index relative to the station of Ain Sefra shows that the SPI goes through a global deficit trend with the existence of many distinct wet and dry periods (Fig. 2). The values of SPI of the study area ranged from -2.608 to 1.986, where the drought years represent 14.28 % of the series (SPI ≤ -1.00), the wet years represent 7.14% (SPI> 1.00), and the near-normal years (-0.99<SPI<0.99) represent 78.57%. In addition, three wet periods were identified, 1967 to 1980, 1987 to 1994, and 2006 to 2012, the year 2008 being highly wet (SPI= 1.99). In contrast, there were three dry periods, 1980 to 1986, 1994 to 2005, and 2012 to 2021, the year 2016 being arid (SPI = -2.61). The most crucial peak for Ain Sefra is negative (SPI= -2.61). Throughout Ain Sefra's chronology, floods have frequently been produced by rainy periods after extended periods of dryness, such as the floods of 1990 (SPI=1.71) and floods of 2008 (SPI=1.99). The main statistical parameters of SPI in the study area are: a value of 1.99 to the max positive, -2.61 to the max negative, 0.58 to the mean positive and -0.76 to the mean negative.

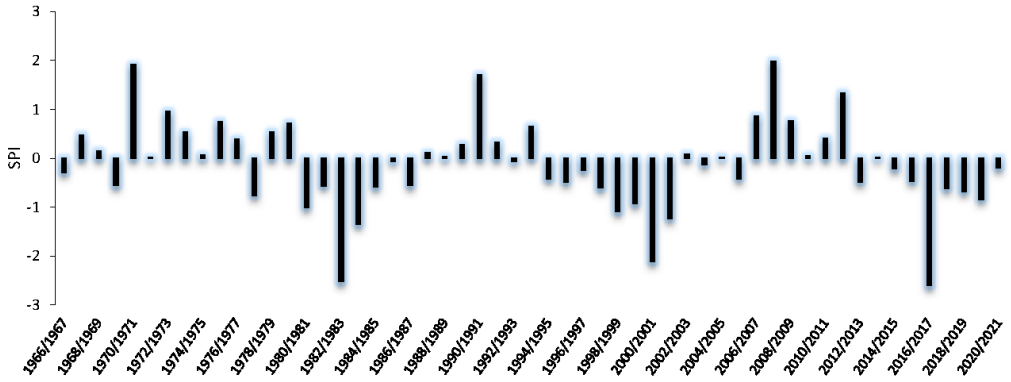

Figure 2. Annual SPI evolution at the study area.

3.1.2. Precipitation Mean Deviation Index (MDX)

The computation of the index of the divergence from the average of the rainfall series at the study area (Fig. 3) makes it possible to show that during this long observation period of 56 years (19662021), there were 48.2% of surplus years and 51.8 % of deficit years. An essential deficit retained from this rainfall series is –146.66 mm recorded in 2020-2021. It is worth remarking here that there are four sequences of a single isolated dry year (1973, 1977, 1992, 2013), one sequence of two successive dry years (2019 to 2021), and three sequences of more than two subsequent dry years (1980 to 1984, 1986 to 1990, 1995 to 2007). The most extended drought sequence was between 1995 and 2007, with 12 consecutive dry years. During 1980-2001, the overall trend is drought, but this is interspersed with a short period with a wet tendency.

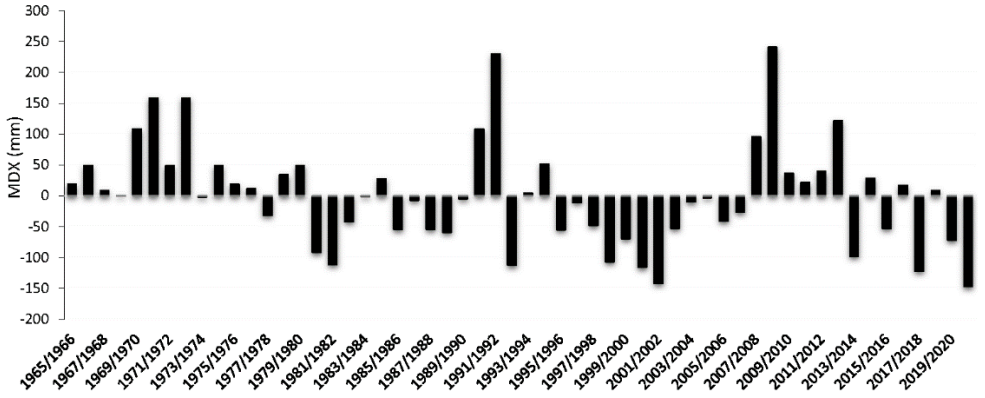

Figure 3. Precipitation Mean Deviation Index at the study area during the monitoring period.

3.1.3. Rainfall Index (RI)

The analysis of drought by the R I and cumulative deviations shows an alternation of sequences with a generally dry trend and arrangements with a naturally wet trend (Fig. 4). The RI values at the study area ranged from -146.66 to 240.33, and the values of varied from -0.72 to 1.19. From 1980 to 1990 and from 1992 to 2007, the overall trend is represented by drought. But it is interspersed with short periods with a wet movement, the most important of which extend over consecutive years (1990 to 1992, 1993 to 1995, and 2008 to 2013). This confirms the findings based on the SPI results.

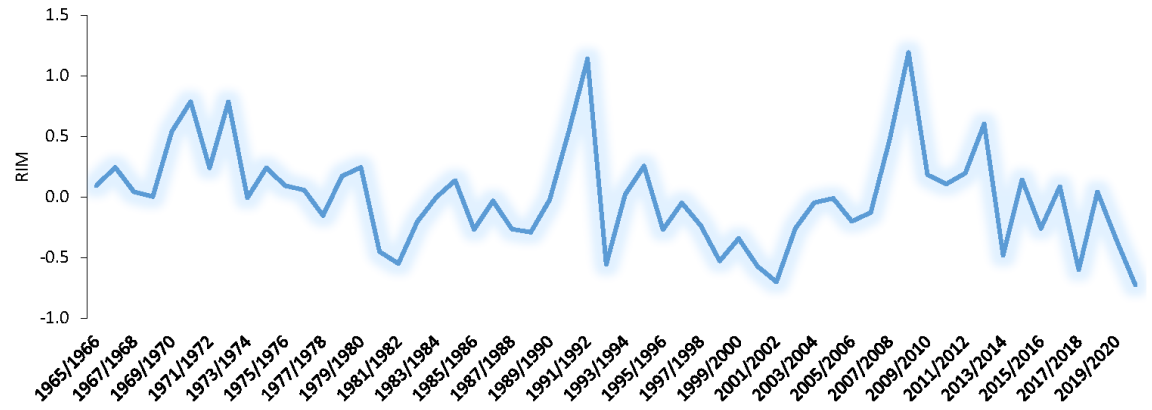

Figure 4. Rainfall Index at the study area during the monitoring period.

3.1.4. Standard deviations Indicator (SDI)

The calculation of the deviation indicator from the average of the rainfall series of the station of Ain Sefra (Fig. 5) makes it possible to show rainfall evolution during this long observation period (56 years from 1966 to2021). Thus, the graphic allows us to distinguish, among the deficit years, 62.50% of years of moderate drought, 10.71% of years of severe drought, and 26.78% of years of very severe drought.

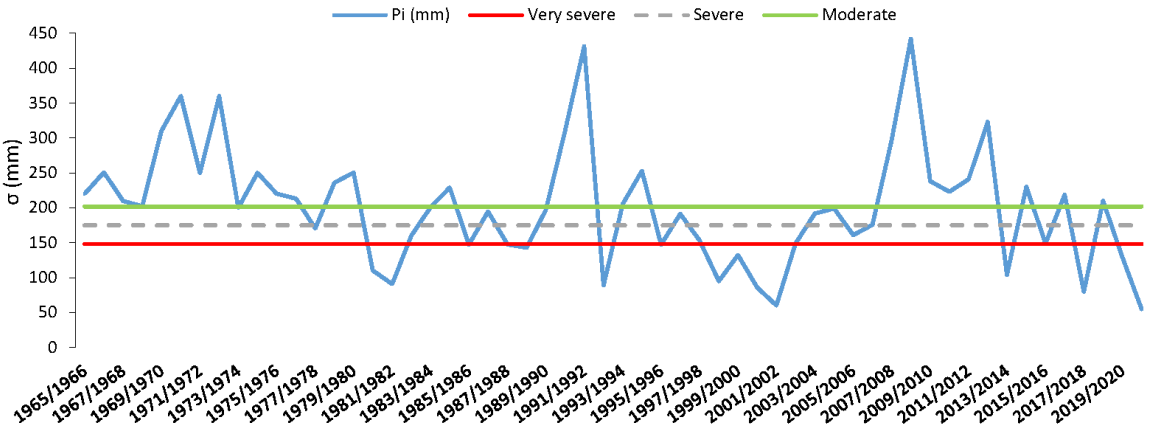

Figure 5. Precipitation Standard Deviation Index at the study area.

3.1.5. Frequency analyses

In this study, dry and wet years have been identified with the MDX and the RI. To better specify the degree of drought recorded, we have used other indices such as the frequency analysis. The application of frequency analysis to the rainfall series of the weather station gave us a higher accuracy for standard years than years with deficit and surplus. Thus, Figure 6 represents variations in annual rainfall in the function of the hydrological years by comparison with the different classes of frequencies. For the station of Ain Sefra, over the 56 years of observation: 7 were very dry, 11 were dry, representing a 32.14% of the series, 15 standard years represented a rate of 26.78%, 11 wet years, and 12 were very wet, representing a 41.07% of the series. We conclude that SPI and the frequency analysis indices have nearly the same results and descriptions based on these results. However, the frequency analysis has more detailed explanations, particularly regarding the standard years concerning SPI and MDX indices. Nevertheless, the frequency analysis does not make it possible to identify the overall trends in rainfall at the level of the station studied.

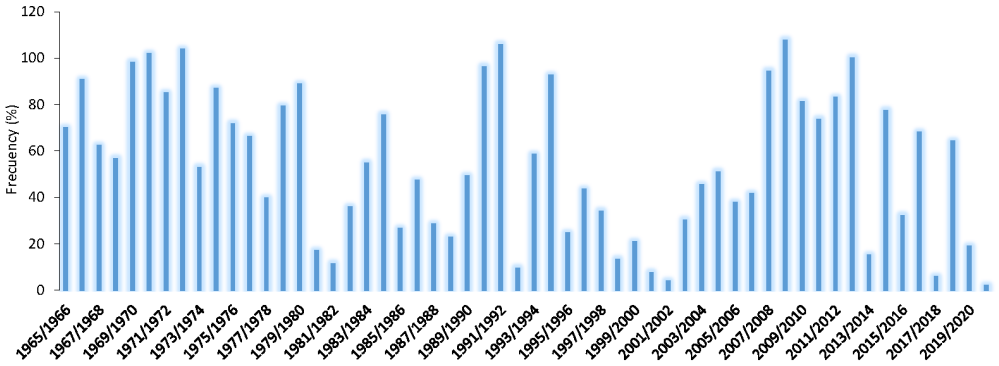

Figure 6. Frequency analysis for the rainfall series at the study area.

3.1.6. Persistence of drought

The drought is perceived more intensively if the year in question follows one or more dry years. A series of consecutive dry years is more severe than a single drought. For the station of Ain Sefra, drought, as determined by the SDI, occurred during three sequence periods and represented by 50% of the entire series, one of 12 years (from 1994 to 2006), the other of 7 years (1980 to 1987), and the third of 9 years (from 2012 to 2021). Following the analysis of the dry years determined by the frequency analysis method at the Ain Sefra station, it was found that there were 18 dry years, where six sequences of a single isolated dry year (1985, 1992, 1995, 2013, 2015, 2017), three sequences of two successive dry years (1980 to 1982, 1987 to 1989, 2019 to 2021) and one sequence of six subsequent dry years (1997 to 2003). For the region, the percentage of an isolated dry year is 10.71%. Sequences of consecutive dry years (two or more) represent 21.43%, according to the analysis of rainfall data from the Ain Sefra station, which characterizes the most representative example of the whole area. Through several drought indices, we can conclude that drought is a recurring phenomenon. A summary of different indices used in this study is given in Table 3.

Table 3. Summary indexes for evaluating droughts at the study area from 1965 to 2021.

	Dry years		**Isolated dry years**		**Successive dry years**	
	Value	**%**	**Value**	**%**	**Value**	**%**
MDX	29	51.78	6	10.71	4	41.07
SPI	8	14.28	3	7.14	1	1.78
RI	29	51.78	6	10.71	4	41.07
FI	18	32.14	6	10.71	4	41.07
SDI	15	26.78	5	8.92	3	26.78

3.2. Diachronic analysis using Remote Sensing

Results of the accomplished diachronic analysis are showed with maps plotting the changes obtained from multi-temporal Landsat images (between 1977 and 2017). The calculation of the MSAVI of the satellite images covering the study area for March 1977,1987, 1997, 2007, and 2017 allowed us to visualize the impact of drought over time (Fig. 7). The confusion matrix was used to evaluate the categorization and plotted in Figures 7 and 8. Thus, the kappa coefficient was employed to measure the classification quality. This matrix indicates the trust level and the main confusion during an image classification (some class pixels can be confused by others). When the kappa coefficient exceeds 0.8 (80%), the classification is considered conventional and relevant. In our study, the kappa value exceeded this threshold of 80% in all the cases (1977: 92.2%; 1987: 96.4%; 1997: 89%; 2007: 83.2%; 2017: 88%). Thus, this statement allowed us to verify our findings. After rigorous examination, it was discovered

that the dynamism of sands in the study area has gone through numerous phases over the five sequences studied (1977, 1987, 1997, 2007, and 2017), ranging from regression to progression. This trend is primarily due to the drought, but other aspects such as wind speed, extensive labor, and overgrazing could also be considered. In general, the sand invasion has increased. This upward trend of sand encroachment has maintained to the present day and represents a serious hazard. Likewise, according to our map examinations, we conclude that the area's sandy accumulations have evolved and become unsteady through time. Maps of the diachronic study have clearly shown that there has been a very significant evolution of sands in terms of area, showing a transition towards the north and the north-east of the study area during the last 56 years (1965-2021), being droughts the main cause from the author's knowledge. In 2017, the sand encroachment massively increased by 286.61% compared with 1977, as in Figure 8, while the vegetation cover category was affected by the type of year, dry or wet. Vegetation cover represented 20.64% of the study area in 2007 in the wet year, where the SPI value was 1.99, and represented only 0.78% of the study area in 1977, where the SPI value was -0.76. The vegetation density decreased considerably in 1997 compared to 1987, owing to consecutive dry years. Table 4 summarizes the evolution of land use components of the study area (1977-2017).

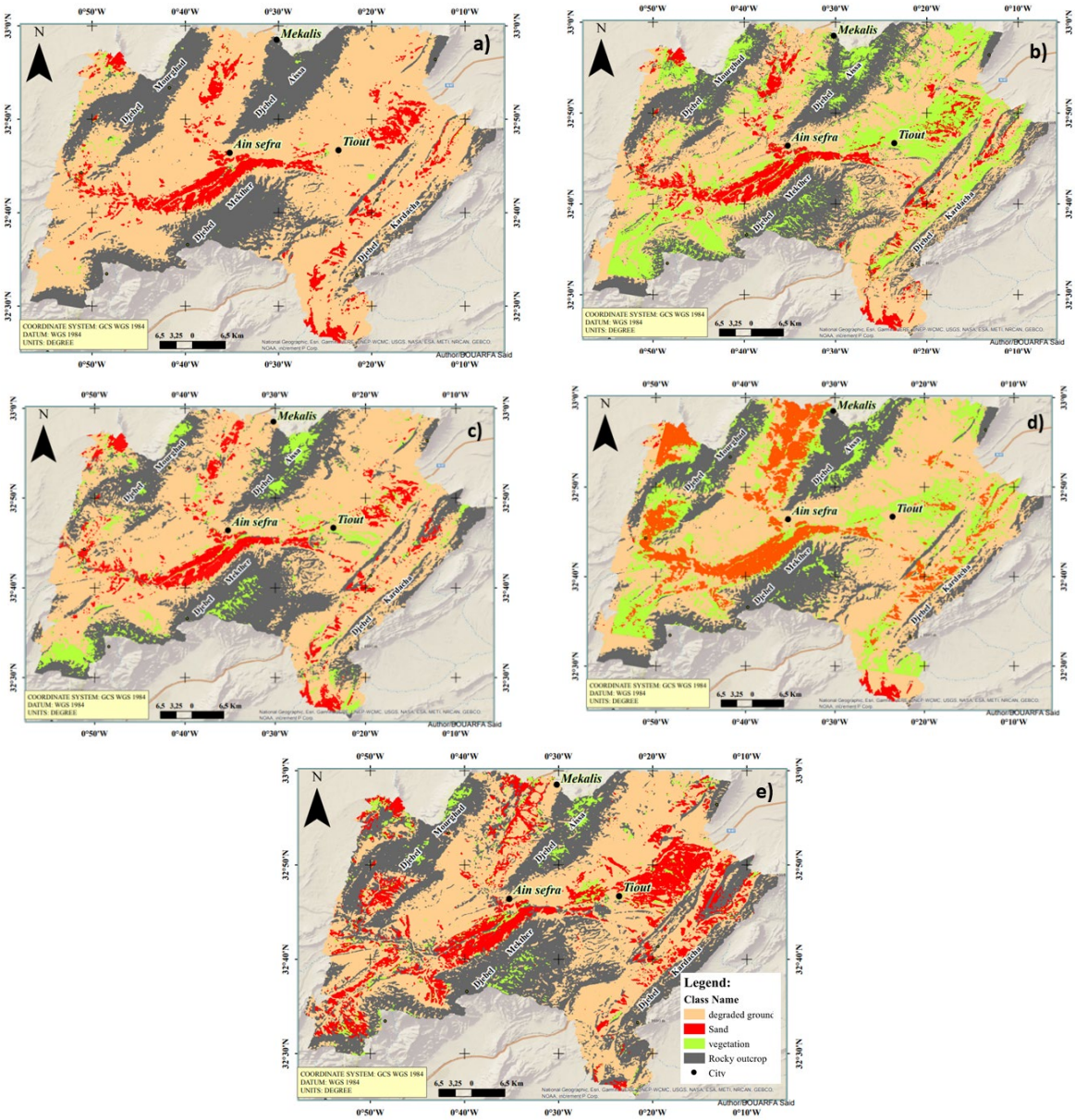

Figure 7. Diachronic Study (a: 1977; b: 1987; c: 1997; d: 2007; e: 2017).

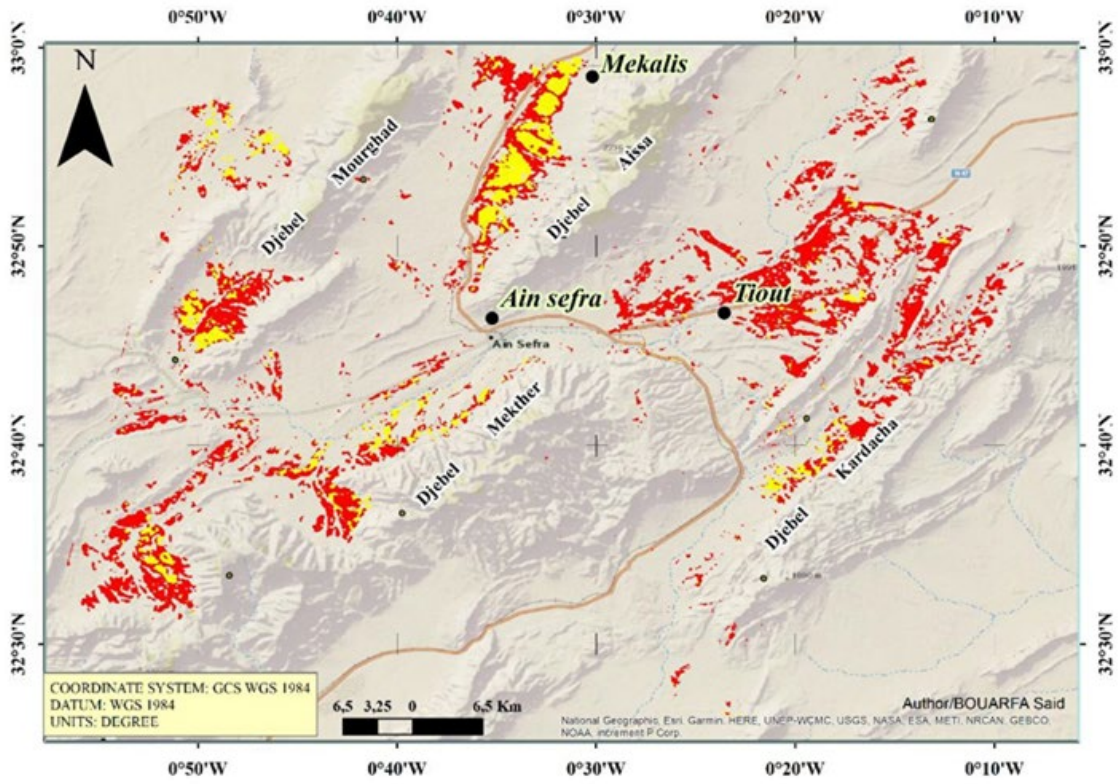

Figure 8. Evolution of sands between 1977 and 2017. Yellow color: new accumulation of sands. Red color: latest dunes higher than 2m.

Table 4. Evolution of land use components of the study area (1977-2017).

		Class (%)		
Year	**Sands**	**Degraded Soils**	**Outcrops**	**Vegetation**
1977	8.29	63.92	27.01	0.78
1987	11.86	40.71	30.72	16.71
1998	12.2	42.03	39.16	6.61
2007	15.66	25.03	38.67	20.64
2017	23.76	40.47	30.41	5.36

4. Conclusions

This paper assessed the potential change in the Ain Sefra region's climate from 1965 to 2021 using, among others, drought indices and remote sensing. The study area is affected by extreme weather events, from droughts to floods. The drought indices used in this study present suitable pictures and perceptions of drought in the research area. The chronological variation of the SPI index relative to the station of Ain Sefra shows that the SPI goes through a global deficit trend with the existence of many distinct wet and dry periods. The values of SPI in the study area range from -2.608 to 1.986, where the most significant peak is negative. Three consecutive dry periods were identified in the first of 7 years (1980 to 1987), the second of 12 years (from 1994 to 2006), and the third of 9 years (from 2012 to 2021), where the year 2016 is arid with an SPI value of -2.61. Contrariwise, three wet periods were distinguished from 1967 to 1980, 1987 to 1994, and 2006 to 2012, where 2008 was highly more west (SPI=1.99). Floods are often caused by wet periods after long consecutive dry periods throughout the history of Ain Sefra, such as the floods of 1990 (SPI=1.71) and floods of 2008 (SPI=1.99). The MDX showed that during this long observation period of 56 years (1965-2021) in Ain Sefra, we had recorded 48.2% surplus years and 51.8% deficit years. The rainfall index showed that the overall trend is represented by drought from 1980 to 1990 and 1992 to 2007. Still, it is interspersed with short periods

with a wet movement, the most important of which extend over consecutive years (1990 to 1992, 1993 to 1995, and 2008 to 2013). According to frequency analyses, over the 56 years of observation: 7 were very dry, 11 were dry, representing 32.14% of the series, 15 standard years represented 26.78%, 11 wet years, and 12 were very wet, representing a 41.07% of the series. The results obtained in this study showed that drought is a recurring phenomenon.

A diachronic assessment was used in the study area to monitor droughts between 1977 and 2017. The MSAVI index of the satellite images covering the study area for March of 1977, 1987, 1997, 2007, and 2017 allowed us to visualize the impact of droughts over time. Following our results plotted as maps, key findings emerge that the area of sandy accumulations has increased in extent and becomes unsteady through time. The maps of the diachronic study have clearly shown that there has been a very significant evolution of sands in terms of area with a transition of it towards the north and the north-east. These issues are mainly related with droughts according to the author's knowledge. This upward trend of sand encroachment has continued to the present day and represents a severe hazard. In 2017, the sand encroachment massively increased by 286.61% compared to 1977. The combination of drought indices and remote sensing seems to be most promising, their findings being valuable tools for supervision and assessment supporting decisions of local and regional authorities.

Acknowledgements

Financial support to perform this study was provided partially by the University Center Salhi Ahmed Naama (Argelia). Antonio Jodar-Abellan acknowledges financial support received form the XTREME Spanish National Project (Ref: PID2019-109381RB-I00/AEI/10.13039/501100011033). In the same way, the authors acknowledge the reviewers and editor of this manuscript whose comments contributed greatly to improve this paper.

References

AghaKouchak, A., Farahmand, A., Melton, F., Teixeira, J., Anderson, M., Wardlow, B. D., Hain, C., 2015. Remote sensing of drought: Progress, challenges and opportunities. *Reviews of Geophysics* 53(2), 452-480. https://doi.org/10.1002/2014rg000456

Bergaoui, M., Alouini, A., 2002. Caractérisation de la sécheresse météorologique et hydrologique: cas du bassin versant de Siliana en Tunisie. *Science et changements planétaires/Sécheresse* 12(4), 205-213.

Boix-Fayos, C., Boerboom, L.G.J, Janssen, R., Martínez-Mena, M., Almagro, M., Pérez-Cutillas, P., Eekhout, J.P.C., Castillo, V., de Vente, J., 2020. Mountain ecosystem services affected by land use changes and hydrological control works in Mediterranean catchments. *Ecosystem Services* 44, 101136. https://doi.org/10.1016/j.ecoser.2020.101136

Bouabdelli, S., Meddi, M., Zeroual, A., Alkama, R., 2020. Hydrological drought risk recurrence under climate change in the karst area of Northwestern Algeria. *Journal of Water Climate Change* 11(S1), 164-188. https://doi.org/10.2166/wcc.2020.207

Bouarfa, S., Abdessamed, D., Okkacha, Y., Almaliki, A.H., Jodar-Abellan, A., Hussein, E.E., 2022a. Sedimentological investigation of the potential origin and provenance of sand deposits in an arid area: a case study of the Ksour Mountains Region in Algeria. *Arabian Journal of Geosciences* 15, 1460. https://doi.org/10.1007/s12517-022-10697-z

Bouarfa, S., Youb, O., Khaouani, B., Berrabah, D., Djoudi, W., 2022b. Assessing Aeolian Sand Potential in Ain Sefra Region-Southwestern of Algeria. *Technium Social Sciences Journal* 30(1), 710-726. https://doi.org/10.47577/tssj.v30i1.6169

Cámara-Artigas, R., de Souza, B.I., de Lima, R.P., 2022. Climatic changes and distribution of plant formations in the state of Paraíba, Brazil. *Cuadernos de Investigación Geográfica* 48, 157-174. https://doi.org/10.18172/cig.5044

Camarasa-Belmonte, A.M., 2021. Flash-flooding of Ephemeral Streams in the Context of Climate Change. *Cuadernos de Investigación Geográfica* 47, 121-142. https://doi.org/10.18172/cig.4838

Corwin, D.L., 2021. Climate change impacts on soil salinity in agricultural areas. *European Journal of Soil Science* 72(2), 842-862. https://doi.org/10.1111/ejss.13010

Cimusa-Kulimushi, L., Bigabwa-Bashagaluke, J., Prasad, P., Heri-Kazi, A.B., Lal Kushwaha, N., Masroor, M.D., Choudhari, P., Elbeltagi, A., Sajjad, H., Mohammed, S., 2023. Soil erosion susceptibility mapping using ensemble machine learning models: A case study of upper Congo River sub-basin. *Catena* 222, 106858. https://doi.org/10.1016/j.catena.2022.106858

Derdour, A., Bouanani, A. 2019. Coupling HEC-RAS and HEC-HMS in rainfall–runoff modeling and evaluating floodplain inundation maps in arid environments: case study of Ain Sefra city, Ksour Mountain. SW of Algeria. *Environmental Earth Sciences* 78(19), 1-17. https://doi.org/10.1007/s12665-019-8604-6

Derdour, A., Bouanani, A., Babahamed, K., 2017a. Floods typology in semiarid environment: Case of Ain Sefra watershed (Ksour mountains, Saharian atlas, SW of Algeria). *Journal of Fundamental and Applied Sciences* (29), 283-299. https://doi.org/10.4314/JFAS.V10I3.29

Derdour, A., Bouanani, A., Babahamed, K., 2017b. Hydrological modeling in semi-arid region using hec-hms model. Case study in Ain Sefra watershed, Ksour mountains (sw-Algeria). J*ournal of Fundamental and Applied Sciences* 9(2), 1027-1049. http://dx.doi.org/10.4314/jfas.v9i2.27

Derdour, A., Mahamat Ali, M. M., Chabane Sari, S. M. 2020. Evaluation of the quality of groundwater for its appropriateness for drinking purposes in the watershed of Naama, SW of Algeria, by using water quality index (WQI). *SN Applied Sciences* 2(12), 1-14. https://doi.org/10.1007/s42452-020-03768-x

Edwards, D.C., Thomas, M.B., 1997. *Characteristics of 20th century drought in the United States at multiple time scales.* Report. Colorado State University, Fort Collins, USA. Available at: https://mountainscholar.org/handle/10217/170176

Eekhout, J.P.C., Boix-Fayos, C., Pérez-Cutillas, P., de Vente, J., 2020. The impact of reservoir construction and changes in land use and climate on ecosystem services in a large Mediterranean catchment. *Journal of Hydrology* 590, 125208. https://doi.org/10.1016/j.jhydrol.2020.125208

Eekhout, J.P.C., Millares-Valenzuela, A., Martínez-Salvador, A., García-Lorenzo, R., Pérez-Cutillas, P., Conesa-García, C., de Vente, J., 2021. A process-based soil erosion model ensemble to assess model uncertainty in climate-change impact assessments. *Land Degradation and Development* 32, 2409-2422. https://doi.org/10.1002/ldr.3920

Eklund, L., Seaquist, J. 2015. Meteorological, agricultural and socioeconomic drought in the Duhok Governorate, Iraqi Kurdistan. *Natural Hazards* 76(1), 421-441. https://doi.org/10.1007/s11069-014-1504-x

Fadhil, A.M., 2011. Drought mapping using Geoinformation technology for some sites in the Iraqi Kurdistan region. *International Journal of Digital Earth* 4(3), 239-257. https://doi.org/10.1080/17538947.2010.489971

Golian, S., Mazdiyasni, O., AghaKouchak, A., 2015. Trends in meteorological and agricultural droughts in Iran. *Theoretical Applied Climatology* 119(3), 679-688. https://doi.org/10.1007/s00704-014-1139-6

Guo, Y., Huang, S., Huang, Q., Wang, H., Fang, W., Yang, Y., Wang, L., 2019. Assessing socioeconomic drought based on an improved Multivariate Standardized Reliability and Resilience Index. *Journal of Hydrology* 568, 904-918. https://doi.org/10.1016/j.jhydrol.2018.11.055

Habibi, B., Meddi, M., Torfs, P. J., Remaoun, M., Van Lanen, H. A., 2018. Characterisation and prediction of meteorological drought using stochastic models in the semi-arid Chéliff–Zahrez basin (Algeria). *Journal of Hydrology: Regional Studies* 16, 15-31. https://doi.org/10.1016/j.ejrh.2018.02.005

Haddouche, I., Toutain, B., Saidi, S., Mederbal, K., 2008. How to reconcile the development of steppe populations and the fight against desertification? Case of the wilaya of Nâama (Algeria). *Food and Agricultural Organization of the United Nations* 7 (3): 25-31. https://agris.fao.org/agris-search/search.do?recordID=QC2013000069

Ibañez, J., Gartzia, R., Alcalá, F.J., Martínez-Valderrama, J., 2022. The Importance of Prevention in Tackling Desertification: An Approach to Anticipate Risks of Degradation in Coastal Aquifers. *Land* 11, 1626. https://doi.org/10.3390/land11101626

IOWA, 2022. IOWA State University, IOWA Enviromental Mesonet: ASOS-AWOS-METAR Data Download. Retrieved from https://mesonet.agron.iastate.edu/request/download.phtml?network=DZASOS&fbclid=IwAR2kyKYKq2gy98a2tBKVSHzlKwHSXgdjovmDHQOdSl_8wmgbkwcmKmmr9YA

Jain, V.K., Pandey, R.P., Jain, M.K., Byun, H.R., 2015. Comparison of drought indices for appraisal of drought characteristics in the Ken River Basin. *Weather Climate Extremes* 8, 1-11 https://doi.org/10.1016/j.wace.2015.05.002

Jodar-Abellan, A., Ruiz, M., Melgarejo, J., 2018. Climate change impact assessment on a hydrologic basin under natural regime (SE, Spain) using a SWAT model. *Revista Mexicana de Ciencias Geológicas* 35 (3), 240-253. http://dx.doi.org/10.22201/cgeo.20072902e.2018.3.564

Jodar-Abellan, A., Fernández-Aracil, P., Melgarejo-Moreno, J., 2019. Assessing Water Shortage through a Balance Model among Transfers, Groundwater, Desalination, Wastewater Reuse, and Water Demands (SE Spain). *Water* 11 (5): 1009-1027. https://doi.org/10.3390/w11051009

Juárez, O., Corbat, M.C., Fucks, E., 2022. Evolución y dinámica geomorfológica de la cuenca del río Amarillo, en el Sistema del Famatina (La Rioja, Argentina). *Revista Mexicana de Ciencias Geológicas* 39, 1. 54-70. http://dx.doi.org/10.22201/cgeo.20072902e.2022.1.1637

Keyantash, J., 2018. *The Climate Data Guide: Standardized Precipitation Index (SPI).* Retrieved from https://climatedataguide.ucar.edu/climate-data/standardized-precipitation-index-spi

Kogan, F., Guo, W., 2016. Early twenty-first-century droughts during the warmest climate. *Geomatics, Natural Hazards Risk* 7(1), 127-137. https://doi.org/10.1080/19475705.2013.878399

Lazri, M., Ameur, S., Brucker, J. M., Lahdir, M., Sehad, M., 2015. Analysis of drought areas in northern Algeria using Markov chains. *Journal of Earth System Science* 124(1), 61-70. https://doi.org/10.1007/s12040-014-0500-6

Li, L., She, D., Zheng, H., Lin, P., Yang, Z.L., 2020. Elucidating diverse drought characteristics from two meteorological drought indices (SPI and SPEI) in China. *Journal of Hydrometeorology* 21(7), 1513-1530. https://doi.org/10.1175/jhm-d-19-0290.1

Malhi, G.S., Kaur, M., Kaushik, P., 2021. Impact of climate change on agriculture and its mitigation strategies: A review. *Sustainability* 13(3), 1318. https://doi.org/10.3390/su13031318

McKee, T.B., Doesken, N.J., Kleist, J., 1993. The relationship of drought frequency and duration to time scales. *Eighth Conference on Applied Climatology.* 17-22. California. Available at: https://www.droughtmanagement.info/literature/AMS_Relationship_Drought_Frequency_Duration_Time_Scales_1993.pdf

Mendoza-Uribe, I., 2022. Identification of changes in the rainfall regime in Chihuahua's state (México). *Cuadernos de Investigación Geográfica* 48, 111-132. https://doi.org/10.18172/cig.5049

Mishra, A.K., Singh, V.P. 2010. A review of drought concepts. *Journal of Hydrology* 391(1-2), 202- 216. https://doi.org/10.1016/j.jhydrol.2010.07.012

Niñerola, A., Ferrer-Rullan, R., Vidal-Suñé, A., 2020. Climate change mitigation: Application of management production philosophies for energy saving in industrial processes. *Sustainability* 12(2), 717. https://doi.org/10.3390/su12020717

Oliveira-Santos, N., Souza-Machado, R.A., Lois-González, R.C., 2022. Identification of levels of anthropization and its implications in the process of desertification in the Caatinga biome (Jeremoabo, Bahia-Brazil). *Cuadernos de Investigación Geográfica,* 48. 41-57. https://doi.org/10.18172/cig.5212

Palacios-Cabrera, T.A., Valdés-Abellán, J., Jódar-Abellán, A., Rodrigo-Comino, J., 2022. Land-use changes and precipitation cycles to understand hydrodynamic responses in semiarid Mediterranean karstic

watersheds. *Science of the Total Environment* 819 (153182), 1-12. https://doi.org/10.1016/j.scitotenv.2022.153182

Qi, J., Chehbouni, A., Huete, A.R., Kerr, Y.H., Sorooshian, S., 1994. A modified soil adjusted vegetation index. *Remote Sensing of Environment* 48(2), 119-126. https://doi.org/10.1016/0034- 4257(94)90134-1

Rahdari, M.R., Rodríguez-Seijo, A., 2021. Monitoring Sand Drift Potential and Sand Dune Mobility over the Last Three Decades (Khartouran Erg, Sabzevar, NE Iran). *Sustainability* 13, 9050. https://doi.org/10.3390/su13169050

Ripple, W.J., Wolf, C., Newsome, T.M., Gregg, J.W., Lenton, T.M., Palomo, I., Duffy, P.B., 2021. World scientists´s warning of a climate emergency 2021. *BioScience* 71(9), 894-898. https://doi.org/10.1093/biosci/biz088

Rodrigo-Comino, J., Salvia, R., Egidi, G., Salvati, L., Giménez-Morera, A., Quaranta, G., 2022. Desertification and Degradation Risks vs Poverty: A Key Topic in Mediterranean Europe. *Cuadernos de Investigación Geográfica* 48 (1), 23-40. https://doi.org/10.18172/cig.4850

Seltzer, P., 1946. *Le climat de l'Algérie.* Inst. Météor. et de phys-du globe. Univ. Alger. 219 pag. Available at: https://www.scirp.org/(S(czeh2tfqyw2orz553k1w0r45))/reference/ReferencesPapers.aspx?ReferenceID=1268152.

Silva, L.F., de Souza, B.I., Cámara, A.R., 2022. Identification of desertified and preserved areas in a conservation unit in the state of Paraíba-Brazil. *Cuadernos de Investigación Geográfica* 48(1), 59-78. https://doi.org/10.18172/cig.5098

Sobral, B.S., de Oliveira-Junior, J.F., de Gois, G., Pereira-Júnior, E.R., de Bodas Terassi, P.M., Muniz-Júnior, J.G.R., Zeri, M., 2019. Drought characterization for the state of Rio de Janeiro based on the annual SPI index: trends, statistical tests and its relation with ENSO. *Atmospheric Research,* 220, 141-154. https://doi.org/10.1016/j.atmosres.2019.01.003

Spinoni, J., Naumann, G., Carrao, H., Barbosa, P., Vogt, J., 2014. World drought frequency, duration, and severity for 1951–2010. *International Journal of Climatology,* 34(8), 2792-2804. https://doi.org/10.1002/joc.3875

Stagge, J.H., Tallaksen, L.M., Gudmundsson, L., Van Loon, A.F., Stahl, K., 2015. Candidate distributions for climatological drought indices (SPI and SPEI). *International Journal of Climatology,* 35(13), 4027-4040. https://doi.org/10.1002/joc.4267

Tahir, F., Ajjur, S.B., Serdar, M.Z., Al-Humaiqani, M., Kim, D., Al-Thani, S.K., Al-Ghamdi, S.G., 2021. *Qatar Climate Change Conference 2021: A Platform for addressing key climate change topics facing Qatar and the world.* Report available at: https://www.academia.edu/66926850/Qatar_Climate_Change_Conference_2021_A_Platform_for_addressing_key_climate_change_topics_facing_Qatar_and_the_world

Thom, H.C.S., 1966. Some methods of climatological analysis. World Meteorological Organization. *Technical Note* nº 81, 69 pages. Available at: https://library.wmo.int/doc_num.php?explnum_id=1961

Tsakiris, G., Vangelis, H., 2004. Towards a drought watch system based on spatial SPI. *Water Resources Management* 18(1), 1-12. https://doi.org/10.1023/b:warm.0000015410.47014.a4

UN, 2022. *Provisional State of the Global Climate 2022*. United Nations (UN). 60 pages. Report available at: https://www.un.org/en/climatechange/reports

USGS, 2022. The USGS *Global Visualization Viewer (GloVis), Landsat Data.* Retrieved from https://glovis.usgs.gov/

Valdes-Abellán, J., Pardo, M.A., Jodar-Abellan, A., Pla, C., Fernandez-Mejuto., M. 2020. Climate change impact on karstic aquifer hydrodynamics in southern Europe semi-arid region using the KAGIS model. *Science of the Total Environment* 723 (138110), 1-9. https://doi.org/10.1016/j.scitotenv.2020.138110

Van Leeuwen, C.C.E., Cammeraat, E.L.H., de Vente, J., Boix-Fayos, C., 2019. The evolution of soil conservation policies targeting land abandonment and soil erosion in Spain: A review. *Land Use Policy* 83, 174-186. https://doi.org/10.1016/j.landusepol.2019.01.018

Wang, G., 2005. Agricultural drought in a future climate: results from 15 global climate models participating in the IPCC. *4th Assessment. Climate dynamics* 25(7), 739-753. https://doi.org/10.1007/s00382-005-0057-9

Wardlow, B.D., Anderson, M.C., Verdin, J.P., 2012. *Remote sensing of drought: Innovative monitoring approaches.* Publisher CRC Press. 484 pages. Available at: https://www.routledge.com/Remote-Sensing-of-Drought-Innovative-Monitoring-Approaches/Wardlow-Anderson-Verdin/p/book/9781138075207#

West, H., Quinn, N., Horswell, M., 2019. Remote sensing for drought monitoring & impact assessment: Progress, past challenges and future opportunities. *Remote Sensing of Environment* 232, 111291. https://doi.org/10.1016/j.rse.2019.111291

Wilhite, D.A., 2000. Drought as a natural hazard: concepts and definitions. In Donald A. Wilhite (Ed.), *Drought: A Global Assessment,* Vol. I, pp. 3–18. Available at: https://digitalcommons.unl.edu/cgi/viewcontent.cgi?article=1068&context=droughtfacpub

Zhang, A., Jia, G., 2013. Monitoring meteorological drought in semiarid regions using multi-sensor microwave remote sensing data. *Remote Sensing of Environment,* 134, 12-23. https://doi.org/10.1016/j.rse.2013.02.023